Ecology shapes the cyclic dominance games between *Escherichia coli* strains

Thierry Kuhn[1], Junier Pilar[1], Redouan Bshary[1], Diego Gonzalez[1,*], Xiang-Yi Li Richter[1,*]

1. Institute of Biology, University of Neuchâtel, Rue Emile-Argand 11, 2000 Neuchâtel, Switzerland
[*]Corresponding authors: D.G. (diego.gonzalez@unine.ch); X-Y.L.R. (li@evolbio.mpg.de)

Abstract

Evolutionary game theory has provided various models to explain the coexistence of competing strategies, one of which is the rock-paper-scissors (RPS) game. A system of three *Escherichia coli* strains—a toxin-producer, a resistant, and a sensitive—has become a classic experimental model for studying RPS games. Previous experimental and theoretical studies, however, often ignored the influence of ecological factors such as nutrients and toxin dynamics on the evolutionary game between the competing strains. In this work, we combine experiments and modeling to study how these factors affect strain coexistence. Using 3D-printed mini-bioreactors, we tracked the community dynamics in different culturing media and under different flow regimes. We found that both nutrients and flow rates impact the population dynamics. In the simulations, we explicitly modeled the release, diffusion, and removal of toxin in space. We showed that the amount of released toxin that is retained in the system is a simple indicator that can predict whether the strains can coexist across broad parameter space. Using the RPS game between the *E. coli* strains as a case study, our work showed the advantage and vast potential of integrating ecology into evolutionary game models for understanding and predicting evolutionary dynamics in biologically realistic contexts.

Introduction

Cyclic dominance interactions represent an interesting type of evolutionary dynamics that have been suggested to promote species coexistence in nature [1–4]. In contrast to hierarchical competition dynamics, where stronger competitors tend to exclude weaker ones, in cyclic dominance interactions, there is no obvious best competitor. Each player can beat some competitors, but loses when confronted to others, like in the children's "rock-paper-scissors" game, where paper wraps rock, rock crushes scissors, and scissors cut paper, forming a dominance circle (Figure 1A). This type of interaction seems less common in animals (yet with famous examples, such as the mating strategy polymorphism in side-blotched lizards [5]), but it is widespread in plants [6–8] and microbial communities where organisms engage in toxin-mediated warfare [1,9–11].

Escherichia coli is a mammalian gut commensal and pathogen that heavily relies on bacteriocidal toxins, collectively named colicins, to exclude conspecific competitors. This bacterium has been used as a model system for studying cyclic dominance both experimentally and theoretically. In the gut, strains that

produce colicins, strains that are sensitive to colicins, and strains that, at some cost, have acquired a resistance to colicins often coexist [12,13]. In such a system, the toxin-producers kill sensitive individuals, the resistant individuals outgrow the toxin-producers, and the sensitive individuals outgrow the resistant ones in pair-wise competitions, which suggests that a “rock-paper-scissors” evolutionary game might underlie the coexistence between the strains (Figure 1AB). Mathematical models and experiments based on this system have identified important factors that determine the likelihood of strain coexistence, including the range of spatial interaction [2], mobility rate [4], spatial heterogeneity [14], and community size [15]. The relative competitiveness between the strains has also been found to play an essential role in determining the evolutionary dynamics, for example, asymmetric competitiveness between the strains may lead to “survival of the weakest”, where the least competitive strain in terms of growth or killing rates consistently dominates the community [11,16–18]. However, previous models and experiments have often neglected the role of some key ecological factors at play in *E. coli's* natural environment, which can dramatically change the competition dynamics between the players in the “rock-paper-scissors” evolutionary game.

The mammalian gut is a complex and dynamic ecosystem in which parameters like pH, nutrient availability, spatial structure, and flow constantly vary, both locally and globally [19]. Some of these parameters, especially nutrients and flow, may influence the competitive interactions between *E. coli* strains by affecting their relative growth rates and the local concentrations of colicin. Because colicins are protein-based toxins, their production is particularly costly and inefficient in environments where amino acids are limiting [20]. The production of colicins is therefore often directly modulated by nutrients, either at the transcriptional level, like in the case of colicin K and E1, which are induced upon starvation, or at the posttranscriptional level, like for colicin E2, whose release is inhibited by glucose [21–23]. The concentration of toxins is also highly sensitive to hydrodynamic factors. Due to their high molecular weight (40 to 80 kDa [20]), the spatial and temporal distributions of colicins can be affected by their varying diffusion rates in the heterogeneous intestinal extracellular matrix [24]. Moreover, the rate of toxin removal, by flow or degradation, can change throughout the gut. Because colicins are potent and fast-acting [20], small changes in toxin concentration could dramatically impact the sensitive strain survival and threaten coexistence between the three strains. However, the effects of toxin removal have rarely been studied as such in mathematical models and are usually not controlled or accounted for in experiments [2,11].

In this work, we combined laboratory experiments and computer simulations to study how the availability of nutrients and the rate of toxin production and removal affect the “rock-paper-scissors” evolutionary game in *E. coli*. Our experiments involved continuous cultures of communities of the three *E. coli* strains in 3D-printed mini-bioreactors with different media compositions and flow rates. To help discriminate between toxin-related and growth-related effects, we built a simulation model that independently controls toxin production, toxin diffusion, and toxin removal on the one hand, and growth parameters on the other

hand. Through stepwise simulations, the model follows population dynamics and toxin levels in a spatially tractable way (Figure 1CD; see also Figure 3AB). It helps understand what the key variables can explain coexistence and competition outcomes in natural environments.

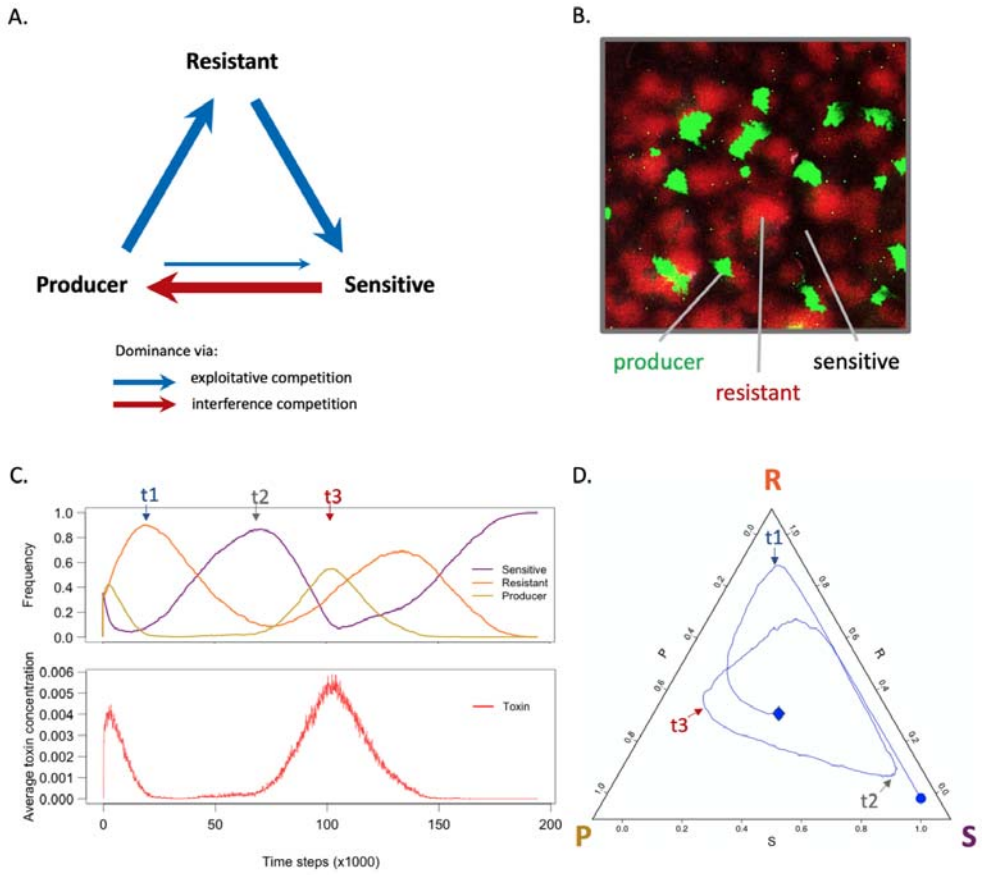

Figure 1. Basic concepts underlying the research. A. Cyclic dominance driven by toxin-mediated killing (i.e., interference competition [25,26], represented by the red arrow) or higher growth rate (i.e., exploitative competition [25,26], represented by the blue arrows) between three *E. coli* strains: a bacteriocidal toxin producer, a toxin-resistant, and a toxin-sensitive strain. B. Micrograph of a multi-strain biofilm on a nutrient agar plate. The producer, resistant and sensitive strains are in green (GFP), red (DsRedExpress) and black, respectively. C. Changes in strain frequency (upper part) and toxin concentration (lower part) as a function of time during a simulation run of the model. In the upper graph, yellow, orange, and purple lines represent the frequencies of the producer, the resistant, and the sensitive strains over time; in the lower graph, the red line represents the toxin concentration (which correlates, with some delay, with the frequency of the producer strain). D. Alternative representation of the strain frequencies shown in panel C as a "ternary plot." The strain frequency changes are represented as a trajectory between three vertices representing each one of the three genotypes: P for the producer, R for the resistant, and S for the sensitive strain. The three timepoints t1, t2, and t3 match between panels C and D. Ternary plot representations will be favored in the main figures of the article.

Materials and Methods

1. The experiments

1.1 3D-printed mini-bioreactor

A mini-bioreactor (Figure 2) was designed using the Autodesk Fusion 360 software and exported as an STL file (provided in the ESM). We also provide detailed CAD drawings of the design in the ESM. It was printed with the BioMed Clear (Formlabs, RS-F2-BMCL-01) resin with a layer height of 0.1 mm using a Formlabs 3b desktop 3D printer. This resin is certified to be biocompatible, water-proof, and autoclavable. The mini-bioreactor has a working volume of 1 mL. The medium is constantly renewed through an inflow connector, connected to a medium dispenser, and an outflow connector, connected to a waste container; the flow of medium is controlled by two pumps, one for the inlet, and one for the outlet. Sterile air supply is ensured by an aeration pipe connected to a 0.22 µm mesh filter. A funnel-shaped sampling chamber capped by a rubber stopper serves for inoculation and sampling purposes.

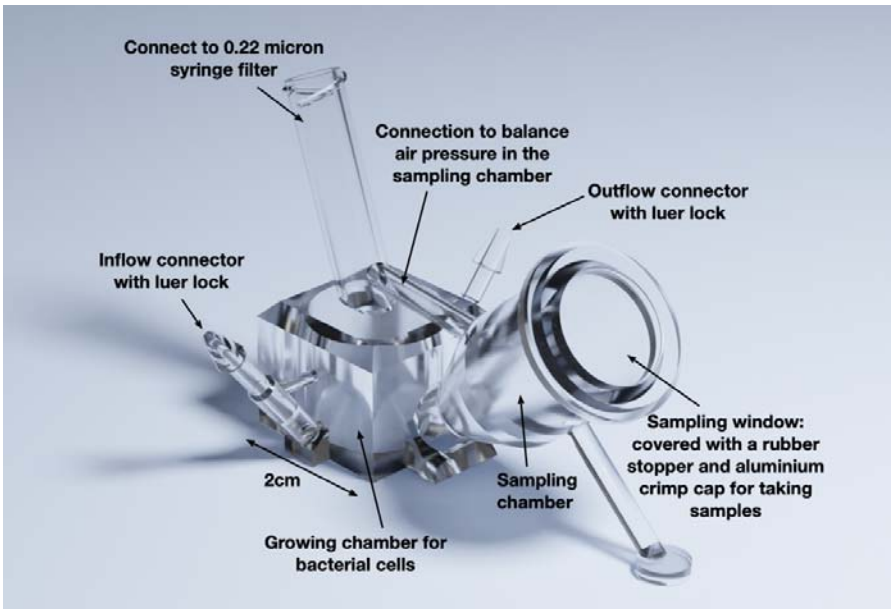

Figure 2. A 3D illustration of the mini-bioreactor used for continuous cultures of the bacterial communities in the experiments.

1.2 Bacterial strains

We use three strains of the bacterium *E. coli*: the BZB1011 pColA strain that harbors the pColA plasmid and produces colicin A (a pore-forming toxin); the BZB1011 *btuB* strain that does not produce the toxin but is resistant to it (mutation in the colicin A receptor BtuB); and the BZB1011 strain that neither produces the toxin nor is resistant to it [27]. The producer and resistant strains are chromosomally tagged with green and red fluorescence proteins, respectively; the cost of those markers has been shown to be negligible [27]. The three strains were cryo-preserved in 30% (v/v) glycerol at -80 °C. To reactivate the bacteria, cells were first plated on the LB agar plates (10g/L Tryptone, Oxoid; 5 g/L NaCl, Sigma-Aldrich;

5 g/L Yeast Extract, Oxoid; 15 g/L Agar, Carl Roth) through polygonal spreading and grown overnight at 37 °C in darkness. We then prepared bacteria suspension from the overnight culture; the three strains were inoculated into liquid LB medium and grew at 37 °C under constant rotation (300 rpm) for 16 hours. After that, the bacterial suspension was centrifuged (5 minutes at 3000G) and then resuspended in physiological water (9 g/L NaCl, Sigma-Aldrich). The bacterial suspension of each strain was adjusted to an optical density (at 600 nm) of 1.0.

1.3 Culturing media

We prepared three culturing media with different proportions of nutrients by supplementing the minimal *E. coli* medium M63-salts [28] with different amounts of Casamino acids (Sigma-Aldrich) and D-glucose (Carl Roth). Casamino acids are hydrolyzed casein, which contains a complex mixture of protein subunits ready for bacteria to transform into cellular building blocks. The media with high, intermediate, and low Casamino acids-to-glucose (CA:G) ratios contained 10 g/L, 3 g/L, and 1 g/L of Casamino acids and 0 g/L, 7 g/L, and 9 g/L of D-glucose, respectively. Growing in the medium with low Casamino acids requires extensive anabolism to lead to protein and lipid biosynthesis. To minimize the potentially deleterious effects of the colicin resistance mutation in poor media, we also added 1.25 mg/L of cobalamin (Fluka) to each medium.

1.4 Quantification of the strain-specific growth rates under different conditions

Cultures of the three genotypes were diluted in the three different culturing media to an optical density of 0.01. The growth of eight 200 µL replicates was monitored in a 96-well-plates incubated at 37 °C with constant agitation for 48 hours in a Bio-Tek Synergy HT microplate reader. The optical density (600 nm) was measured once an hour. The growth rates were calculated based on data recorded during the exponential growth phase.

1.5 Experimental conditions and continuous culturing of the bacterial communities

We implemented a factorial design of three different culturing media and two dilution speeds for a total of six different experimental conditions. Five replicates of the bacterial communities (each in a separate mini-bioreactor) were prepared for each experimental condition. We used two multi-channel peristaltic pumps (Longer, LP-BT100-1L) to control the inflow and outflow of the media into and out of each mini-bioreactor. The inflow rate was set to either 250 µL/h (high flow rate) or 100 µL/h (low flow rate); the outflow was kept at a constant pumping speed of 1 mL/h. Because the outlet of the mini-bioreactor was placed higher than the inlet, having a higher pumping speed at the outlet ensures sufficient air exchange and a constant volume of 1 mL in the mini-bioreactors. After connecting the mini-bioreactors, we flushed them with 100 mL fresh medium at maximum pumping speed to prevent contamination. Finally, we mixed the cell suspensions of each strain in equal proportions and pipetted 50 µl of the mixed bacterial suspensions into each mini-bioreactor by shortly removing the air filter. The mini-bioreactors were kept at 37 °C in the darkness for 14 days.

1.6 Quantification of the bacterial community composition

The relative abundances of the three *E. coli* strains in each mini-bioreactor were quantified each weekday during the two weeks of experiments. A 150 µL sample was taken using a sterile syringe (1 mL, Codan) with a needle (Ø0.6 × 60 mm, Sterican) through the rubber stopper on the sampling window of each mini-bioreactor. The sample was centrifuged for 5 minutes at 2000 x g and 145 µL of the supernatant was removed. The cells were then resuspended in the rest 5 µL of the medium and placed on an agar pad. We then took pictures of the agar pad under a microscope (Leica DM4 B) in sets of three — a phase contrast picture, a picture with the GFP settings, and a picture with the RFP settings. For each sample, we took at least two pictures at different random positions on the agar pad with at least 60 cells in each picture. The pictures were then analyzed using the FIJI software (version 2.3.0, [29]) with the StarDist 2D plugin [30] to count cells of different colors. We also manually checked the results of the automatic cell detection and corrected possible detection errors in each picture.

2. The simulation model

2.1 Model overview

To help better understand the experimental results, we designed a spatially explicit, individual-based simulation model. Our model was based on a 200×200 lattice with periodic boundaries, where each position contained information about the toxin concentration and its spatial occupation by at most one bacterial cell (Figure 3). We considered three bacterial cell types, corresponding to the colicin-producing, resistant, and sensitive strains of *E. coli* we used in the experiments. To initiate the simulation, we populated 1% of the positions in the lattice with a bacterium chosen at random among the three strains. The toxin concentration was set to zero everywhere. In each of the subsequent time points, we updated every position of the lattice following the order of (i) cell death and removal, (ii) toxin concentration dynamics (including the production, diffusion, and removal of colicin), and (iii) colonization of the empty positions by cell growth. The simulations were stopped either when coexistence was lost (i.e., only one cell type was left) or when they reached 300’000 steps. We implemented the model using the *Julia* programing language. The simulation codes are available from the corresponding authors upon request.

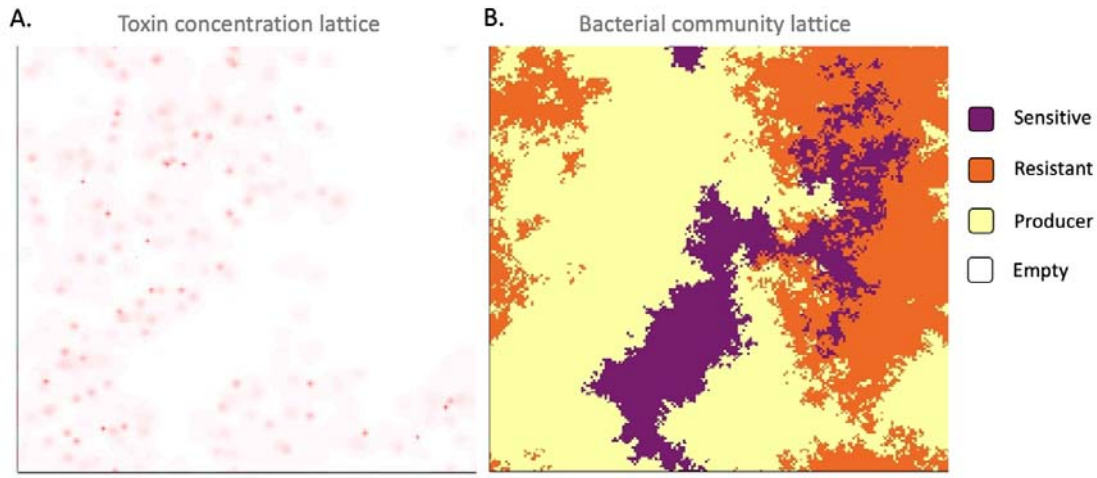

Figure 3. An illustration of the simulation model. Panels A and B show the toxin concentration and spatial occupation of bacterial cells in the lattice, respectively. The state of the simulation corresponds to timepoint t3 in Figure 1CD.

2.2 Simulation of cell death

Cells of different types can die due to different causes. Besides a baseline death probability (d_0) that we assumed to be identical for all cell types, the colicin-producing cells can also die from spontaneous lysis to release colicin, and the sensitive cells may be killed by colicin in the local environment. Because the resistant strain neither produces, nor can be killed by, colicin, its death probability $d_R = d_0$. The death probability of the colicin-producing strain $d_P = d_0 + d_l$, where d_l denotes the spontaneous lysis probability that was set to a positive constant. In contrast to the constant death probabilities of colicin-producing and resistant cells, the death probabilities of sensitive cells are spatially and temporally heterogeneous and depend on the local colicin concentration. We denote the death probability of a sensitive cell at location (i, j) as $d_{S_{i,j}} = d_0 + kc(x_{i,j}, t)$, where k is a positive constant. The death probability $d_{S_{i,j}}$ is a linearly increasing function of the local colicin concentration c at the position $x_{i,j}$ at time step t. At each time step, all bacterial cells on the lattice may die at their corresponding strain- and location-specific probabilities. The death events occurred in random order, and the dead cells were removed to leave an empty space on the lattice.

2.3 Simulation of toxin concentration dynamics

The lysis of every colicin-producing cell releases an equal amount of colicin into the environment. The concentration dynamics of colicin are controlled by a set of partial differential equations

$$\frac{\partial c(x_{i,j}, t)}{\partial t} = P(x_{i,j}, t) - uc(x_{i,j}, t) + D\nabla^2 c(x_{i,j}, t), \qquad \text{(Eq. 1)}$$

where $P(x_{i,j}, t)$ is the production rate of colicin, which equals a positive constant, p, if a colicin-producing cell was located at $x_{i,j}$ and just died at the current time step t; otherwise, it equals 0. The second term on

the right-hand side of Eq. 1 describes the removal of colicin due to the bulk flow of culturing medium. Different values of the colicin removal rate u correspond to different medium flow rates that we implemented in the experiments. We assume that the spontaneous degradation rate of colicin is negligible relative to its removal by medium flow. The diffusion rate D in the last term of Eq. 1 controls the diffusion of colicin between close-by positions in the lattice. The value of D could be affected by factors such as the molecular mass of different colicin molecules and the pore size distribution in the biofilm where the cells are located. Assuming that colicin diffusion occurs at much faster rates than the death and division rates of bacterial cells, we can calculate the quasi-steady-state colicin distribution at time t by setting Eq. 1 to zero and solve for $c(x_{i,j}, t)$. We took the two-dimensional finite difference approximation of Eq. 1 and solved the 200×200 linear system using Fourier transformations following the methods in [31]. In the simulation model, the diffusion rate D is scaled so that it equals the fraction of colicin that diffused from one position to any of the four direct neighboring positions in the lattice at each time step. When $D = 1$, the colicin concentration is averaged over all positions at every time step.

2.4 Simulation of cell growth by colonizing empty spaces

A distinct feature of our model in contrast to typical existing lattice models of "rock-paper-scissors" games (reviewed in [32]) is the way that we modeled growth. We did not allow cells of one type to replace any other type directly; instead, the growth of cells was space-limited, corresponding to exploitative competition where space is the limiting resource, such as in typical biofilms. To grow, a cell has to have access to an empty position among the eight positions in its direct neighborhood (i.e., the Moore neighborhood [33]). Its probability of reproduction is a function of its own growth rate and the occupancy of the cells surrounding the position it attempts to divide into. Practically, for each empty position surrounded by at least one cell, the probability of this position becoming occupied by a colicin-producing, resistant, or sensitive cell was determined by the fraction of the strain's summed growth rates over the summed growth rates of all bacterial cells in the Moore neighborhood of the empty space. The strain-specific growth rate of sensitive cells was set to $r_S = 1$. Because toxin production and resistance cost resources that can be used otherwise for growth, we assumed that the growth rate of the resistant strain $r_R = r_S - v_R$ and the growth rate of the toxin-producing strain $r_P = r_S - v_R - v_P$, where v_R and v_P represent the cost of colicin resistance and production, respectively. A cell cannot reproduce twice during the same timestep.

Table 1. Parameters implemented in the simulation model.

d_0	Baseline per time step death probability of cells
d_l	Spontaneous lysis probability of the toxin-producing cells per time step
D	Diffusion rate of colicin
u	Removal rate of colicin by the flow of culturing medium
r_S	Growth rate of colicin sensitive cells

v_R	Cost on growth rate for colicin resistance
v_P	Cost on growth rate for colicin production
k	Killing rate of sensitive cells by colicin-induced cell lysis
p	Amount of toxin released when a producer cell lyses

Results

1. Experimental results

1.1 Growth rates of the three E. coli strains in different culturing media

Before studying the competition dynamics between the three *E. coli* strains, we first confirmed that their growth rates in monoculture fitted the requirements of a "rock-paper-scissors" game in the three different media used ("high CA:G," "intermediate CA:G," and "low CA:G"). We found that in all nutrient conditions, the sensitive strain had the highest growth rate, followed by the resistant strain, and by the colicin-producing strain. All pairwise comparisons between the growth rate distributions were still significant ($p < 0.001$) after using the Bonferroni correction for multiple comparisons (Figure 4). The average cell doubling times of the *E. coli* strains are shown in Appendix Figure S1. Because of the relatively low nutrient availability in all the culturing media, the doubling times were longer than the typical 20 minutes in rich medium but probably shorter than in the wild [34]. While strains grew faster with higher CA:G ratio, the numerical growth rate difference between the strains was relatively consistent across different nutrient conditions, with a growth rate increment of 0.020 ± 0.005 from the colicin-producing strain to the resistant strain, and an increment of 0.018 ± 0.009 from the resistant strain to the sensitive strain. The relative growth rate difference between the toxin-producing and sensitive strains, however, decreased as the CA:G ratio increased in the medium. The growth rate of the colicin producer strain was 22.0% less than the sensitive strain in the medium with the lowest CA:G ratio, and it was only 14.5% less in the medium with the highest CA:G ratio. This result is consistent with a reduction of colicin-producing cost in richer media, suggesting that the fraction of colicin-producing strains that lyse to release toxin might have decreased as the CA:G ratio increased in the medium. [34]

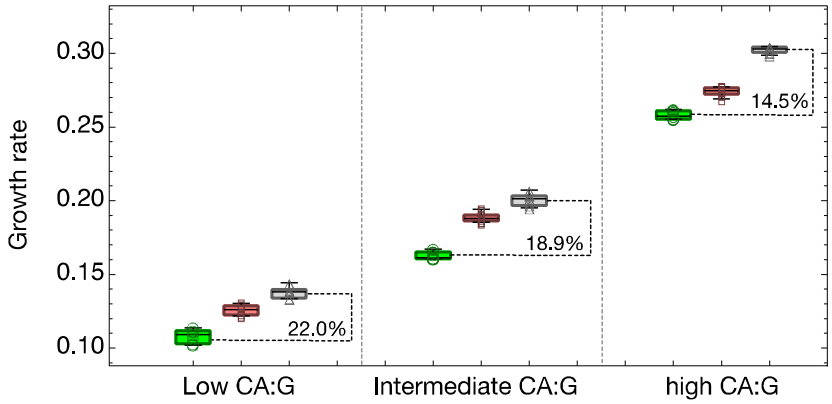

Figure 4. The growth rates of three *E. coli* strains under different nutrient conditions. The box-whisker charts filled with green, red, and gray colors and marked with circle, square, and triangle markers represent

the toxin-producer, the resistant, and the sensitive strains, respectively. The boxplot center lines show the mean, box limits show upper and lower quartiles, whiskers show the 1.5x interquartile range, and each marker corresponds to the result of an independent replicate. We have eight replicates for each bacterial strain and culturing medium combination.

1.2 Effects of nutrient and flow regime on the competition dynamics of E. coli strains

We next followed the population dynamics of the three *E. coli* strains in the three different media and under two different flow regimes (slow and fast) for two weeks in the 3D-printed mini-bioreactors. We found consistent effects of the nutrient condition and the flow regime on the community composition trajectories (Figure 5). In the high CA:G ratio medium, the producer dominated the competition, making up more than 80% of the bacterial population over the entire duration of the experiments after the first day, but neither the resistant nor the sensitive strain became extinct. In contrast, the resistant and sensitive strains appeared more competitive in the medium with low CA:G ratio, where the producer never reached more than 10% of the population. In the medium with intermediate CA:G ratio, the competition outcomes were variable among the replicates, suggesting that the overall competitivities of the three strains were closer in this nutrient environment.

Besides the marked effect of the nutrient environment, the effect of the medium flow rate on the competition dynamics was also noteworthy. In the medium with low CA:G ratio, the flow rate determined which between the resistant and sensitive strain dominated the competition in the time window of our experiments: while a higher flow rate favored the sensitive strain, a lower flow rate favored the resistant strain. This result could be caused by different colicin removal rates. A higher flow rate would give an advantage to the sensitive cells by removing the toxin more quickly. The competition dynamics under low flow rate in the medium with intermediate CA:G ratio were most interesting: all replicates followed a consistent community composition trajectory over time, but the trajectories of different replicates strongly diverged from one another. This suggests that the slightly different initial community composition caused by stochasticity in the inoculation or during the first hours of the experiments may have strongly impacted the subsequent evolutionary trajectories. This could happen if the overall competitiveness of the three strains were in a much closer range under this experimental condition than in the other conditions we tested.

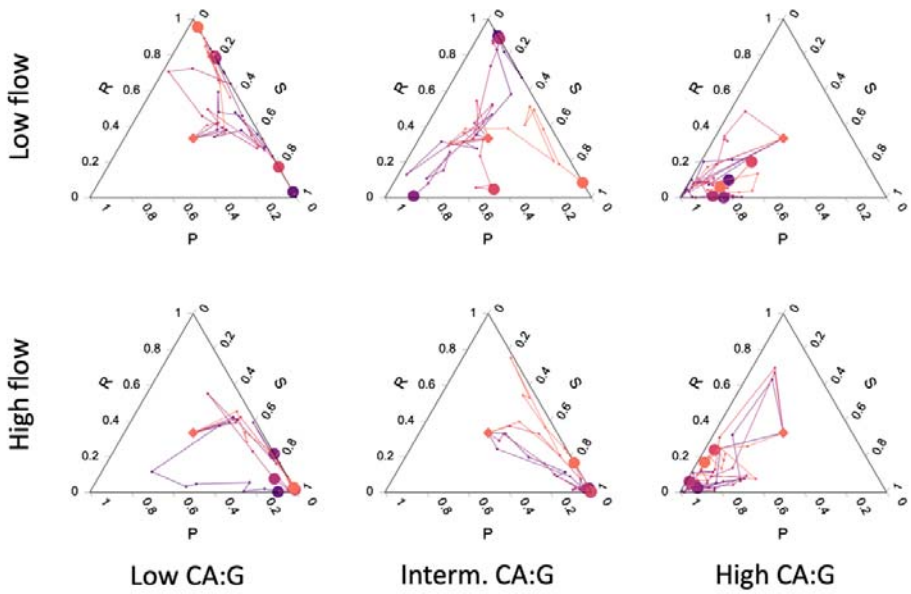

Figure 5. Ternary plots of the community composition of three *E. coli* strains over two weeks in three different media and under two different flow regimes. The frequency of each strain at each time point can be read on the respective side of the ternary plot. Five independent trajectories were plotted in different colors under each condition. The starting point of all trajectories is marked by a diamond; the end point of each trajectory is marked with a circle.

2. Simulation results

2.1 <u>Slower toxin diffusion tends to promote strain coexistence, but up to a limit</u>

To explore in more detail the impact of diffusion, flow, and growth rate on the population dynamics of the three *E. coli* strains, we designed and implemented a spatially explicit model of bacterial toxin-based cyclic competition. We first assessed the impact of toxin diffusion on the coexistence of the three competing strains. The simulations tended to produce longer coexistence times when slower toxin diffusion rates were used (Figure 6; Figure S2). Very short coexistence and no cyclic dominance were characteristic of the instantaneous toxin diffusion case, which is equivalent, when it comes to the toxin concentration, to a well-mixed environment (Figure 6, $D = 1.0$). Because, in this case, sensitive cells are killed at random over the entire lattice, the toxin gives the same advantage to the resistant as to the producer cells; since the resistant cells grow faster than the producer, the resistant wins whenever the toxin reaches concentrations sufficient to eradicate the sensitive and the sensitive wins whenever they do not. With slower diffusion rates, the sensitive population becomes less affected overall by the same amount of released toxin because it takes more time for it to reach patches of sensitive cells; however, in this case, the dying sensitive cells are more often located at the interface with producer patches, which helps the latter strain conquer new space and gives it a colonization advantage. Nevertheless, below a certain toxin diffusion threshold, coexistence breaks down again: the toxin does not diffuse fast enough to free space around the growing producer patch and to help its population increase in frequency. Coexistence is therefore only possible at intermediate toxin diffusion rates.

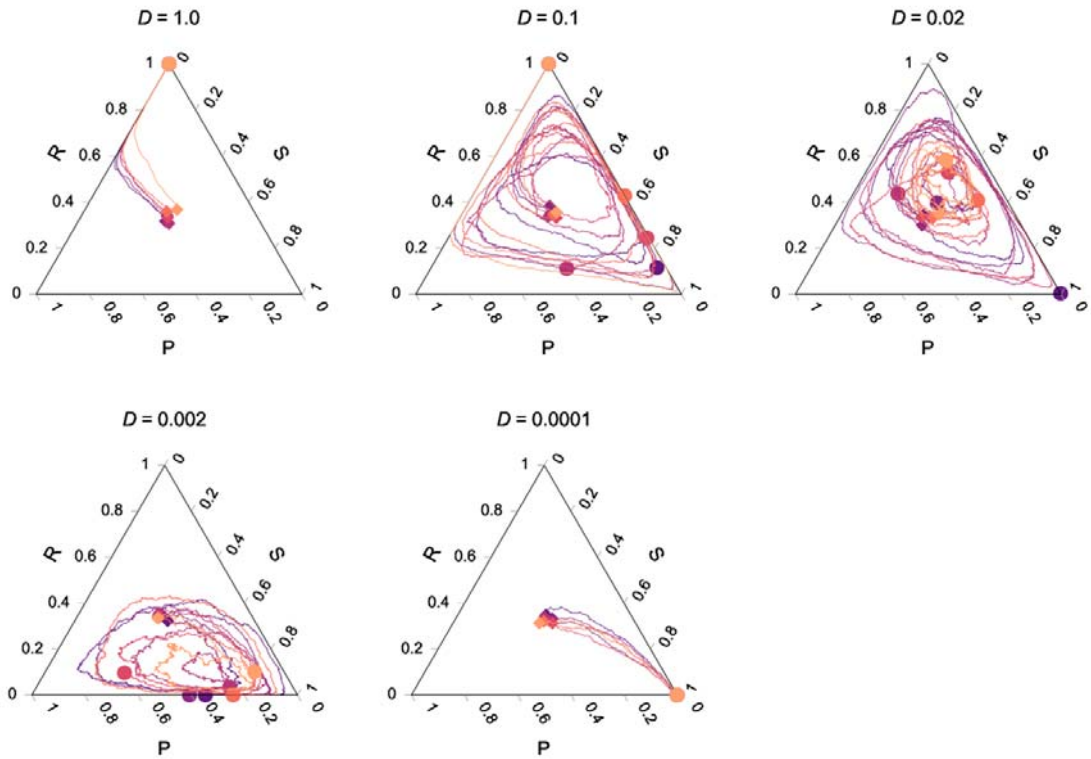

Figure 6. Competition dynamics between the three *E. coli* strains at different toxin diffusion rates (*D*). Very high ($D = 1.0$) and very low ($D = 0.0001$) toxin diffusion rates were detrimental to the colicin-producing strain. At intermediate diffusion rates, the frequencies of the three *E. coli* strains fluctuate in cycles that can be more or less favorable to one of the three strains. The spontaneous lysis rate of the colicin producers and the removal rate of colicin were set to intermediate values: $d_l = 10^{-4}$, and u =0.015. Six independent simulation trajectories were plotted in different colors under each condition. The start point and end point of each trajectory are marked with a diamond and a circle of the same color as the trajectory, respectively.

2.2 Strain coexistence is favored at intermediate toxin accumulation

The levels of toxin in the system are controlled by the producer lysis rate (d_l), which correlates with toxin release, and by the toxin removal rate (u) through medium flow. Both parameters can impact the concentration of toxin in the system, as can be observed in a community consisting of the colicin producer strain only (Figure 7A; Supplementary Figure S3): decreasing d_l and increasing u both lead to lower toxin levels in the system. Although toxin does not reach a steady state in populations comprising all three strains because the producer frequency fluctuates over time, the amount of the toxin contributed by each producer cell which is retained in the system (or "toxin retention"), $pd_l(1-u)$, hereafter denoted as c^*, nonetheless controls toxin accumulation in the system. Our simulations showed that long-term coexistence is favored at intermediate c^* levels. When the values of c^* were too high, like in the cases of low or medium flow rates ($u = 0.0075$ or $u = 0.015$) in combination with high toxin release rates (d_l=3e-4)

(Figure 7B), most of the sensitive cells were killed at the very beginning of the simulations runs, and the producer was subsequently outcompeted by the resistant strain. In such cases, coexistence broke down quickly, with either the resistant or the sensitive strain (if some sensitive cells happen to survive the initial colicin wave) dominating the entire population while the other two strains went extinct. In contrast, when the values of were too low, like in the cases of high or medium flow rates (or) in combination with low toxin release rate (e-5) (Figure 7B), the colicin producers were not able to maintain a toxin level that was high enough to kill sensitive cells. Consequently, the sensitive strain, which has the highest growth rate, excluded the other two strains. Only when was kept within an intermediate range, cyclic population dynamics could emerge, and the coexistence of the strains could be maintained for a relatively long duration.

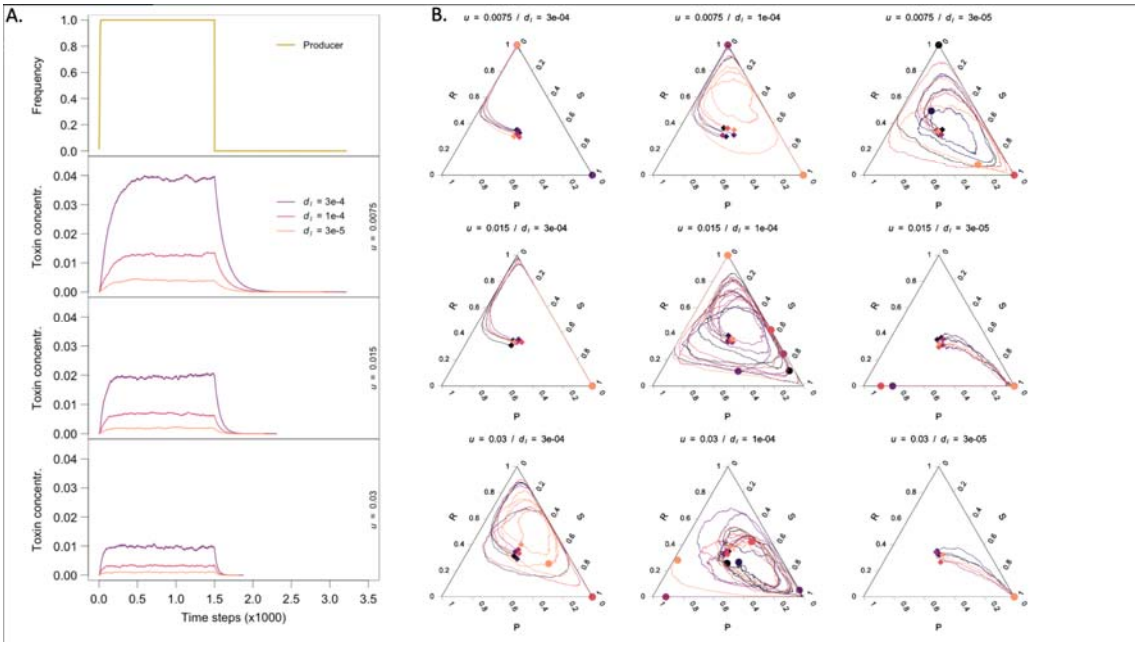

Figure 7. The impact of toxin accumulation on population dynamics. A. Toxin accumulation and toxin removal in a producer population at different toxin production and removal rates. A producer population was left to occupy the entire space for 1500 time steps and then eliminated; toxin increase and decrease (until it reaches the 1e-7 threshold) is observed. Three elements emerge that could affect the strain population dynamics: (1) the toxin steady-state level (plateau), which is the resultant of both production and removal rates and seems to have the highest impact on coexistence, (2) the toxin accumulation rate when the producer population is growing, mainly impacted by the toxin production rate, and (3) the toxin concentration decrease rate when the producer population plummets, mainly impacted by the toxin removal rate. B. Population trajectory for the nine combinations of toxin production and removal rates we used in panel A. The toxin diffusion rate is set to fast (D=0.1); the plots for instantaneous (D=1.0) and slow (D=0.02) diffusion rates can be found in Supplementary Figure S4 for comparison. There are six independent simulation trajectories under each condition, indicated by lines of different colors. The start point and end point of each trajectory are marked with a diamond and a circle of the same color as the

trajectory, respectively. Toxin production rate d_l=3e-5, 1e-4, 3e-4; toxin removal rate u=0.0075, 0.015, 0.03.

2.3 Extreme toxin fluxes can lead to population fluctuations that break down coexistence

Although the lysis rate of the colicin producers d_l and the removal rate of toxin u can both influence the accumulation of colicin in the system, their effects on the competition dynamics between the bacterial strains are not entirely interchangeable. The former controls how fast colicin can accumulate in the system (Figure 7A, colicin concentration rose faster at higher d_l values); the latter controls how fast colicin can be flushed out (Figure 7A, colicin concentration returned to zero faster at higher u values). At the bacterial population level, d_l determines the speed of the sensitive strain collapse when the producer frequency starts to increase, whereas u determines if and when the sensitive strain can bounce back from a toxin wave after the producer's frequency has declined. To show the effects of d_l and u without confounding effects, we adjusted these two parameters correlatively while maintaining the toxin retention, c^*, constant (Figure 8; Supplementary Figure S5). At too low and too high d_l and u values, long-term coexistence between the strains was compromised. In the former case, the toxin was not removed fast enough at the onset of the competition and the sensitive strain was heavily hit by the initial toxin wave leading to the dominance of the resistant strain (or rarely, after a bounce-back, the sensitive strain) over the producer. At too high d_l and u values, the toxin could not be accumulated to a high enough concentration to threaten the sensitive population at the onset of the competition, which then favored the sensitive strain (or sometimes the producer) at the expense of the resistant strain. Such extreme toxin fluxes, through their effect on the sensitive population, increase the probability for one of the three strains to be outcompeted at the very beginning of the competition and for coexistence to break down. Under intermediate toxin production and removal rates, by contrast, the fluctuations of toxin levels were damped, which limited the amplitude of changes in the sensitive and producer populations density and the risk of global disbalance that it entails. Both toxin accumulation and toxin flux need therefore to be within an intermediate range to support long-term strain coexistence.

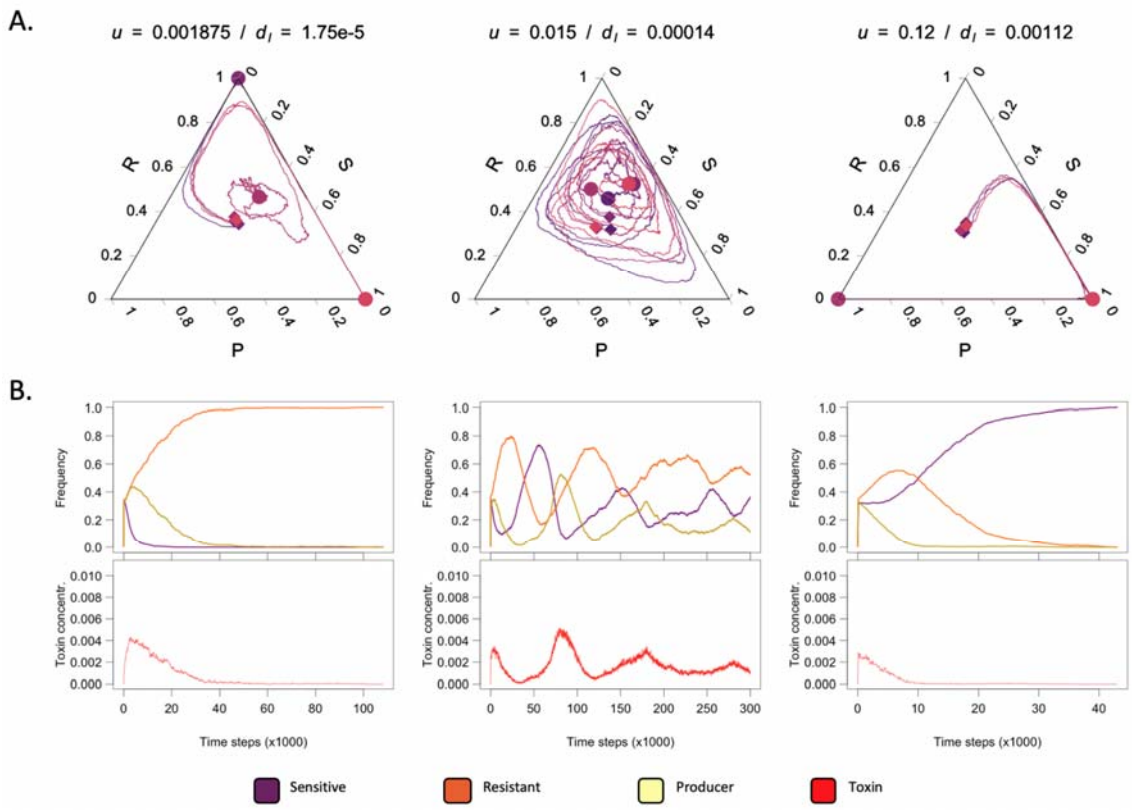

Figure 8. The impact of toxin flux on population dynamics. A. Impact of increasing flow and toxin production on cyclic competition patterns with the toxin retension, , kept constant. There are four independent simulation trajectories under each condition, indicated by lines of different colors. The start point and end point of each trajectory are marked with a diamond and a circle of the same color as the trajectory, respectively. B. Dynamics over time of the three strains and the toxin levels for one of the four replicates. Diffusion rate D = 0.02.

2.4 The individual and population components of toxin production cost affect competition dynamics in similar ways

In the colicin system, the toxin production cost has two components: the cost, paid by all cells, of carrying the toxin producing gene ( ), which lowers the growth rate, and the cost of random cell lysis ( ) that is needed for toxin release. While the first type of cost slows down the growth and affects competition primarily at the edge of growing patches, the second type of cost increases the death rate randomly over the entire population and multiplies foci of toxin release. To test how these two types of cost affected the system, we ran the model in two ways while keeping constant: 1. by varying the cost of carrying the toxin gene ( ), while maintaining the growth rates of the sensitive and the resistant strains unchanged; 2. by varying the lysis rate of the toxin-producing strain ( ) together with the amount of toxin released per lysis event (p). Increasing any of the two types of toxin production cost had similar effects: the center of the population trajectories shifted towards the corner of the sensitive strain in the ternary plots, making it more likely for the sensitive than for the resistant to win the competition (Figure S6). However,

modifications of the second type of cost had a much stronger effect on population dynamics than the first when the overall cost ($v_P + d_l$) were considered. This is because increasing the lysis frequency and decreasing the amount of toxin released, even when keeping the value of c^* identical, changes the toxin distribution over the lattice and thereby profoundly affects the capacity of the producer to interfere with the sensitive strain.

2.5 Varying the relative growth rates between competing strains can influence the competition outcome

Finally, we used our simulation model to test the potential consequences of differences in growth rates between strains in the range of the ones we observed in the experimental part (Figure 4). We ran simulations with the same parameters as in Figure 7B, but with smaller or larger differences in relative growth rates between the three strains by changing the cost of resistance (v_R) and of toxin production (v_P). To support lasting coexistence, lower growth rate differences needed to be compensated by a decrease in the expected retention of toxin contributed by each producer cell, c^*; on the contrary, with higher growth rate differences between the strains, coexistence would generally require higher c^* (Figure S7). This indicates that ecology-driven changes in the relative growth rates between strains, like the ones we observed between the three media in our experimental system, could lead to differences in competition outcome and population dynamics.

Discussion

In this work, we use lab experiments and individual-based simulations to study how relevant ecological factors affect the competition dynamics and coexistence between toxin-producing, toxin-resistant, and sensitive *E. coli* strains. This experimental system is used as a model for cyclic dominance in the "rock-paper-scissors" evolutionary game. The main ecological factors and processes we considered are the impact of resources (i.e., amino acids and glucose) on growth and the accumulation, diffusion, and removal of toxin, which are known to be key variables in *E. coli's* natural environment. The different nutrient conditions we tested by changing the CA:G ratio could emulate aspects of *E. coli*'s biphasic lifestyle inside and outside hosts [35,36] or mimic a commensal *vs* pathogenic adaptation [37,38]. In complex environments like the mammalian gut, diffusion and flow greatly vary depending on growth conditions, especially on whether cells are in a planktonic or in a sessile state within a biofilm [39,40]. Viscosity is known to promote the maintenance of high levels of toxin production in colicinogenic strains because it ensures producer cell assortment [41], but most likely also because it slows down diffusion and increases the benefit of toxin production as our model shows (Figure 6).

In our experiments, the most dramatic difference in competition outcome was due to the nutrients: while the toxin producer dominated under high CA:G, it was largely outcompeted under lower CA:G. To understand this result, it is important to observe that the *E. coli* system of cyclic dominance is fueled by two different types of competition: 1. exploitative competition, which is competition for a shared resource (e.g. nutrients) and plays a major role in the interactions between sensitive and resistant and between

resistant and producer strains; 2. interference competition, which occurs when one competitor directly harms another, like when the producer secretes toxins to kill the sensitive strain. These two types of competition present very different dynamics and respond very differently to ecological factors [25,26]. The timescale of competition is typically long for exploitative competition, whose effect, in our system, requires several generations, while it is short for interference competition, since sensitive cells can be decimated within minutes once a toxin concentration threshold is reached. In the high CA:G medium, the density of all strains, including toxin producers, are higher, leading to higher overall toxin concentrations. Moreover, the relative growth rate differences between the colicin producer and the resistant strains are also smaller in this condition. The combined effect likely helped the colicin producer strain to outcompete the sensitive strain more easily in the medium with high CA:G ratio. Nevertheless, we expect that the resistant cells remaining in communities in the high CA:G medium would eventually take over the dominance if we followed the competition dynamics for a longer duration.

A feature of our work is to focus on the biological relevance of our experimental system and model design. Instead of implementing serial transfers of colonies like in previous experimental studies of the "rock-paper-scissors" dynamics [2,11], we designed and 3D-printed mini-bioreactors where we can keep the competing community in continuous culture. This, for example, allowed us to observe the effect of the toxin remaining in the system on the competition dynamics after the producer population had disappeared (Figure 5, low CA:G, low flow). By catching the "ghost of the colicin producers", we were able to explain the counterintuitive result that the resistant strain increased in frequency in competition with the sensitive strain for several days under low medium flow rate after the population of the producer strain had crashed. In previous simulation models, because toxin was rarely modeled explicitly, mobility of individuals was often introduced to allow cells at some distance to interact with each other. The models have produced interesting results, such as intermediate mobility promotes coexistence [4,45], and long-distance mobility tends to cause coexistence to break down [46,47]. The way mobility was modeled was often by swapping the position of two cells or swapping the position of a cell and an empty space. It is still controversial whether those types of movement may occur in microbial biofilms, where the extracellular polymeric substances build up a matrix-like structure that limits the free movement of cells. In our model, we did not allow the cells to move, and all interactions were through the diffusion of toxin. Our finding that intermediate toxin diffusion rate promotes coexistence draws an analogy to the previous finding that intermediate mobility of individuals promotes coexistence, but is more biologically relevant and has important implications. For example, while we know that spatial structure promotes coexistence in the *E. coli* system [2,11,48], the fact that population structure without restricted toxin diffusion does not support coexistence has not been sufficiently emphasized.

It is often challenging to predict the competition dynamics and outcome between multiple interacting species in complex environments where ecological factors and processes can influence the relative competitiveness between organisms. Recently, it has been found that fairly accurate predictions of the

behavior of such complex systems can be achieved by some simple rules [42]. In our work, we found that what we called toxin retention (c^*), which is determined by the balance between toxin release and removal, is a useful simple indicator of the propensity of long-term coexistence between the *E. coli* strains. We found that intermediate c^* generally promotes coexistence, although extreme toxin fluxes caused by extreme toxin release and removal rates can lead to strong population fluctuations and premature collapse of coexistence. Such simple indicators, if widely applicable, can be very useful in predicting the behavior of cyclic competition dynamics in complex natural environments. We therefore encourage empirical tests in other communities where species interact in "rock-paper-scissors" games.

Evolutionary game theory, through its development in the last 50 years since the seminal work of Maynard Smith and Price [49] that opened up this field, has provided great convenience for modeling and helping us understand complex evolutionary scenarios. Classic evolutionary game models, however, often rely on simple assumptions that ignore the mechanisms underlying the strategies, and do not consider how they might be influenced by ecological factors and processes. Because theoretical studies of evolution have been more advanced than their empirical counterpart in the early days of evolutionary game theory, simple assumptions such as the "phenotypic gambit" [50] were often necessary. However, we should not forget that ecology sets up the theatre for the evolutionary play [51,52], and evolutionary game models should not ignore ecological details. Nowadays, empirical studies of ecology and evolution are much more advanced, thanks to new technological developments like the sequencing and manipulation of genetic materials, convenient analysis of biochemical molecules and their properties, as well as 3D printing that allows us to build customized devices quickly at low costs. Theoreticians also have gained access to new analytical tools and unprecedented computational power. Equipped with these new tools and accumulating knowledge in both the empirical and theoretical studies of ecology and evolution, it should be our new goal to integrate mechanisms underlying evolutionary strategies into the models for the development of evolutionary game theory in the future.

Acknowledgement

We would like to thank Camille Tinguely and Valentin Voegeli for helpful discussions, and Céline Terrettaz for support with the experiments. The study is funded by the Swiss National Science Foundation grant PZ00P3_180142 to D.G. and grant PZ00P3_180145 to X-Y.L.R, and the Novartis Foundation for medical-biological Research grant 19A023 to D.G.

References

1. Czárán TL, Hoekstra RF, Pagie L. 2002 Chemical warfare between microbes promotes biodiversity. *Proceedings of the National Academy of Sciences* **99**, 786–790.
2. Kerr B, Riley MA, Feldman MW, Bohannan BJM. 2002 Local dispersal promotes biodiversity in a real-life game of rock–paper–scissors. *Nature* **418**, 171–174.
3. Kirkup BC, Riley MA. 2004 Antibiotic-mediated antagonism leads to a bacterial game of rock–paper–scissors in vivo. *Nature* **428**, 412–414.

4. Reichenbach T, Mobilia M, Frey E. 2007 Mobility promotes and jeopardizes biodiversity in rock-paper-scissors games. *Nature* **448**, 1046–1049.
5. Sinervo B, Lively CM. 1996 The rock–paper–scissors game and the evolution of alternative male strategies. *Nature* **380**, 240–243.
6. Taylor DR, Aarssen LW. 1990 Complex competitive relationships among genotypes of three perennial grasses: implications for species coexistence. *The American Naturalist* **136**, 305–327.
7. Cameron DD, White A, Antonovics J. 2009 Parasite–grass–forb interactions and rock–paper–scissor dynamics: predicting the effects of the parasitic plant *Rhinanthus minor* on host plant communities. *Journal of Ecology* **97**, 1311–1319.
8. Soliveres S *et al.* 2015 Intransitive competition is widespread in plant communities and maintains their species richness. *Ecology Letters* **18**, 790–798.
9. Stubbendieck RM, Straight PD. 2016 Multifaceted interfaces of bacterial competition. *Journal of Bacteriology* **198**, 2145–2155.
10. Granato ET, Meiller-Legrand TA, Foster KR. 2019 The evolution and ecology of bacterial warfare. *Current Biology* **29**, R521–R537.
11. Liao MJ, Miano A, Nguyen CB, Chao L, Hasty J. 2020 Survival of the weakest in non-transitive asymmetric interactions among strains of E. coli. *Nature Communications* **11**, 6055.
12. Gordon DM, Riley MA, Pinou T. 1998 Temporal changes in the frequency of colicinogeny in *Escherichia coli* from house mice. *Microbiology (N Y)* **144**, 2233–2240.
13. Riley MA, Gordon DM. 1999 The ecological role of bacteriocins in bacterial competition. *Trends in Microbiology* **7**, 129–133.
14. Schreiber SJ, Killingback TP. 2013 Spatial heterogeneity promotes coexistence of rock-paper-scissors metacommunities. *Theoretical Population Biology* **86**, 1–11.
15. Müller APO, Gallas JAC. 2010 How community size affects survival chances in cyclic competition games that microorganisms play. *Physical Review E* **82**, 52901.
16. Frean M, Abraham ER. 2001 Rock–scissors–paper and the survival of the weakest. *Proceedings of the Royal Society B* **268**, 1323–1327.
17. Neumann G, Schuster S. 2007 Continuous model for the rock–scissors–paper game between bacteriocin producing bacteria. *Journal of Mathematical Biology* **54**, 815–846.
18. Nahum JR, Harding BN, Kerr B. 2011 Evolution of restraint in a structured rock–paper–scissors community. *Proceedings of the National Academy of Sciences* **108**, 10831–10838.
19. Miller BM, Liou MJ, Lee J-Y, Bäumler AJ. 2021 The longitudinal and cross-sectional heterogeneity of the intestinal microbiota. *Current Opinion in Microbiology* **63**, 221–230.
20. Cascales E, Buchanan SK, Duché D, Kleanthous C, Lloubes R, Postle K, Riley M, Slatin S, Cavard D. 2007 Colicin biology. *Microbiology and Molecular Biology Reviews* **71**, 158–229.
21. Götz A, Lechner M, Mader A, von Bronk B, Frey E, Opitz M. 2018 CsrA and its regulators control the time-point of ColicinE2 release in *Escherichia coli*. *Scientific Reports* **8**, 6537.
22. Yang T-Y, Sung Y-M, Lei G-S, Romeo T, Chak K-F. 2010 Posttranscriptional repression of the cel gene of the ColE7 operon by the RNA-binding protein CsrA of *Escherichia coli*. *Nucleic Acids Research* **38**, 3936–3951.
23. Ghazaryan L, Tonoyan L, Ashhab A al, Soares MIM, Gillor O. 2014 The role of stress in colicin regulation. *Arch Microbiol* **196**, 753–764.
24. Sandrin D *et al.* 2016 Diffusion of macromolecules in a polymer hydrogel: from microscopic to macroscopic scales. *Physical Chemistry Chemical Physics* **18**, 12860–12876.
25. Cornforth DM, Foster KR. 2013 Competition sensing: the social side of bacterial stress responses. *Nature Reviews Microbiology* **11**, 285–293.
26. Lang JM, Benbow ME. 2013 Species interactions and competition. *Nature Education Knowledge* **4**, 8.
27. Gonzalez D, Sabnis A, Foster KR, Mavridou DAI. 2018 Costs and benefits of provocation in bacterial warfare. *Proceedings of the National Academy of Sciences* **115**, 7593 – 7598.
28. Ausubel FM, Brent R, Kingston RE, Moore DD, Seidman JG, Smith JA, Struhl K, editors. 2003 *Current Protocols in Molecular Biology*. John Wiley & Sons, Inc.
29. Schindelin J *et al.* 2012 Fiji: an open-source platform for biological-image analysis. *Nature Methods* **9**, 676–682.
30. Schmidt U, Weigert M, Broaddus C, Myers G. 2018 Cell Detection with Star-Convex Polygons. *Medical Image Computing and Computer Assisted Intervention - MICCAI 2018 - 21st International Conference, Granada, Spain, September 16-20, 2018, Proceedings, Part II* , 265–273.

31. Doekes HM, de Boer RJ, Hermsen R. 2019 Toxin production spontaneously becomes regulated by local cell density in evolving bacterial populations. *PLoS Computational Biology* **15**, e1007333.
32. Szolnoki A, Mobilia M, Jiang L-L, Szczesny B, Rucklidge AM, Perc M. 2014 Cyclic dominance in evolutionary games: a review. *Journal of the Royal Society Interface* **11**, 20140735.
33. Durrett R, Levin SA. 1994 Stochastic spatial models: a user's guide to ecological applications. *Philosophical Transactions of the Royal Society B* **343**, 329–350.
34. Gibson B, Wilson DJ, Feil E, Eyre-Walker A. 2018 The distribution of bacterial doubling times in the wild. *Proceedings of the Royal Society B* **285**, 20180789.
35. van Elsas JD, Semenov A v, Costa R, Trevors JT. 2011 Survival of *Escherichia coli* in the environment: fundamental and public health aspects. *The ISME Journal* **5**, 173–183.
36. Ihssen J, Egli T. 2005 Global physiological analysis of carbon-and energy-limited growing Escherichia coli confirms a high degree of catabolic flexibility and preparedness for mixed substrate utilization. *Environmental Microbiology* **7**, 1568–1581.
37. Chang D-E *et al.* 2004 Carbon nutrition of *Escherichia coli* in the mouse intestine. *Proceedings of the National Academy of Sciences* **101**, 7427–7432.
38. Alteri CJ, Smith SN, Mobley HLT. 2009 Fitness of *Escherichia coli* during urinary tract infection requires gluconeogenesis and the TCA cycle. *PLoS Pathogens* **5**, e1000448.
39. Flemming H-C, Wingender J. 2010 The biofilm matrix. *Nature Reviews Microbiology* **8**, 623–633.
40. Maunders E, Welch M. 2017 Matrix exopolysaccharides; the sticky side of biofilm formation. *FEMS Microbiology Letters* **364**, fnx120.
41. le Gac M, Doebeli M. 2010 Environmental viscosity does not affect the evolution of cooperation during experimental evolution of colicigenic bacteria. *Evolution (N Y)* **64**, 522–533.
42. Reichenbach T, Mobilia M, Frey E. 2008 Self-organization of mobile populations in cyclic competition. *Journal of Theoretical Biology* **254**, 368–383.
43. Rulquin C, Arenzon JJ. 2014 Globally synchronized oscillations in complex cyclic games. *Physical Review E* **89**, 32133.
44. Zhang G-Y, Chen Y, Qi W-K, Qing S-M. 2009 Four-state rock-paper-scissors games in constrained Newman-Watts networks. *Physical Review E* **79**, 62901.
45. Hol FJH, Voges MJ, Dekker C, Keymer JE. 2014 Nutrient-responsive regulation determines biodiversity in a colicin-mediated bacterial community. *BMC Biology* **12**, 68.
46. Friedman J, Higgins LM, Gore J. 2017 Community structure follows simple assembly rules in microbial microcosms. *Nature Ecology & Evolution* **1**, 109.
47. Holdridge EM, Cuellar-Gempeler C, terHorst CP. 2016 A shift from exploitation to interference competition with increasing density affects population and community dynamics. *Ecology and Evolution* **6**, 5333–5341.
48. Jensen AL. 1987 Simple models for exploitative and interference competition. *Ecological Modelling* **35**, 113–121.
49. Maynard Smith J, Price GR. 1973 The logic of animal conflict. *Nature* **246**, 15–18.
50. Grafen A. 1984 Natural selection, kin selection and group selection. In *Behavioural Ecology: An Evolutionary Approach* (eds JR Krebs, NB Davies), pp. 62–84. Blackwell Scientific.
51. Hutchinson GE. 1965 *The Ecological Theater and the Evolutionary Play*. Yale University Press.
52. Post DM, Palkovacs EP. 2009 Eco-evolutionary feedbacks in community and ecosystem ecology: interactions between the ecological theatre and the evolutionary play. *Philosophical Transactions of the Royal Society B* **364**, 1629–1640.